

Location deterministic biosensing from quantum-dot-nanowire assemblies

Chao Liu,¹ Kwanoh Kim,² and D. L. Fan^{1,2,a)}

¹Materials Science and Engineering Program, Texas Materials Institute, University of Texas at Austin, Austin, Texas 78712, USA

²Department of Mechanical Engineering, University of Texas at Austin, Austin, Texas 78712, USA

(Received 21 May 2014; accepted 12 August 2014; published online 28 August 2014)

Semiconductor quantum dots (QDs) with high fluorescent brightness, stability, and tunable sizes, have received considerable interest for imaging, sensing, and delivery of biomolecules. In this research, we demonstrate location deterministic biochemical detection from arrays of QD-nanowire hybrid assemblies. QDs with diameters less than 10 nm are manipulated and precisely positioned on the tips of the assembled Gold (Au) nanowires. The manipulation mechanisms are quantitatively understood as the synergetic effects of dielectrophoretic (DEP) and alternating current electroosmosis (ACEO) due to AC electric fields. The QD-nanowire hybrid sensors operate uniquely by concentrating bioanalytes to QDs on the tips of nanowires before detection, offering much enhanced efficiency and sensitivity, in addition to the position-predictable rationality. This research could result in advances in QD-based biomedical detection and inspires an innovative approach for fabricating various QD-based nanodevices. © 2014 AIP Publishing LLC.

[<http://dx.doi.org/10.1063/1.4893878>]

In the last decade, considerable research interest was focused on applying semiconductor quantum dots (QDs) for bioimaging,^{1,2} sensing,³ and therapeutic delivery^{4,5} due to their tunable sizes and unique optical properties.⁶ Compared to traditional organic dyes, semiconductor QDs exhibit higher fluorescent brightness and better resistance to photobleaching due to the quantum confinement effect and chemical stability. The emission of QDs can be systematically tuned from the visible to infrared optical regime by varying the sizes and material compositions. The wide absorption band and large Stokes shifts make it possible to stimulate QDs of different colors simultaneously by a single excitation source for optical barcoding of biomolecules.^{7,8} These unique properties were explored for imaging and tracking extracellular events, including cellular motility,^{9,10} protease activity,^{11,12} and signal transduction.^{13,14} They were also applied as nanosensors in an intracellular setting for detection of viruses,^{15,16} cytokines,^{17,18} and pH variations.¹⁹ Nevertheless, the applications of QDs as extracellular biosensors were still largely conducted in bulk colloidal suspensions, which present considerable difficulties in sensing a minute amount of bioanalyte. A breakthrough was made by Wang *et al.*,³ who innovatively coupled fast optical detection, FRET of QD-organic dye hybrids, and microfluidics for unambiguous sorting DNA molecules at a concentration as low as 0.48 nM. Although sensitive and specific, such a method relies on the optical detection of fast flowing QDs and thus requires complex optical instrumentation. It is highly desirable if the QDs can be registered at designated locations for position-predictable optical analysis and sensing.

In this work, we investigate controllable manipulation and assembling of QD-nanowire hybrid nanostructures in suspension by electric fields and applied the assemblies for location deterministic biochemical detection. By applying an

external AC electric field (*E*-field) on the designed microelectrodes, we precisely manipulated and positioned biofunctionalized semiconductor QDs on the tips of aligned Au nanowire arrays. The manipulation mechanism was quantitatively understood and attributed to a synergetic effect of DEP and ACEO. The as-obtained QD-nanowire hybrids operate uniquely by actively focusing bioanalytes to QDs with the *E*-field, followed by biodetection after the *E*-field removal, which offered substantially improved detection efficiency with a sensitivity of 20 nM (Cy5 labeled biotin molecules), in addition to the position deterministic rationality. This work could be a critical step towards a rational bottom-up approach for fabricating various QD-based biomedical devices.

Au nanowires (NWs) (300 nm in diameter, 5 μm in length), fabricated by electrodeposition into nanoporous templates,²⁰ were assembled into aligned arrays by *E* fields and applied for attracting and positioning QDs. Water soluble CdSe/ZnS QDs (525 nm in emission, Invitrogen Inc.) were used for the investigation. The QD-nanowire hybrids were manipulated and assembled in a polydimethylsiloxane (PDMS) well in deionized (D.I.) water by an AC *E*-field with a frequency of 50 kHz to 2 MHz generated from strategically designed interdigital microelectrodes (gaps of 20–50 μm). The *E*-field was controlled by a waveform generator (Agilent 33250 A) and the peak to peak voltage was set at 20 V.

Upon application of the *E*-field, randomly suspended Au NWs (concentration: $2.2 \times 10^7/\text{ml}$) were swiftly attracted, aligned and assembled on the patterned microelectrodes as shown in supplementary material S1.²⁰ The chaining lengths of Au NWs depend on the applied AC frequency.²¹ At 70 kHz, a single layer of nanowires can be formed with an average length of 5.46 μm (supplementary material S1a).²⁰ The length monotonically increased with the AC frequency and reached an average value of 12.33 μm at 800 kHz (supplementary material S1d).

^{a)}Email: dfan@austin.utexas.edu

The transportation and assembling of nanowires can be attributed to the dielectrophoretic (DEP) forces, resulting from the interactions between the E -field and the electrically polarized nanoentities.²² For a nanowire, which can be approximated as a prolate ellipsoid, the DEP force is given by²³

$$F = p \cdot \nabla E = \frac{1}{3} \pi r^2 L \epsilon_m \text{Re}(K) \nabla E^2, \quad (1)$$

where $p = \frac{2}{3} \pi r^2 L \epsilon_m \text{Re}(K) E$ is the induced dipole moment on nanowires, r and L are the radius and length of nanowires, ϵ_m is the dielectric constant of the medium, and $\text{Re}(K)$ is the real part of Clausius-Mossotti factor of the nanowire. The transport and alignment orientations of nanowires were along the directions of the E -field gradient and the E -field, respectively.²⁴ The distinct degree of the chaining effect at different AC frequencies (supplementary material S1e) is due to the unique electric interactions among polarized nanowires, where the electric dipole moment p is a frequency dependent factor. The chaining force between two polarized nanoparticles (F_c) is proportional to E^2 ($F_c \sim E^2$).²⁵ The number of chained particles, simplified as spheres, can be calculated according to $N = c \sqrt[3]{p_{eff}}$, where c is a constant and p_{eff} is the effective electric polarization moment.²³ The value of p_{eff} highly depends on the electric properties of the nanowires and the suspension medium, as well as the quality of the electric contact between neighboring nanoparticles. In our experiments, we can readily align and assemble a layer of single nanowires on the edges of the microelectrodes at 70 kHz and 20 V.

Next, the assembled nanowires were applied for positioning the semiconductor QD nanosensors. We dispersed the QDs (0.1 nM) in the suspension of the assembled Au nanowires in an AC E -field of 50 kHz and 20 V. As soon as the E -field was applied, the QDs coherently moved and circulated from the edges to the top of the microelectrodes, and some docked on the tips of nanowires,²⁰ the QDs transported on top of the microelectrode away from the electrode edges and moved upward (blurred image) until disappeared]. An array of QDs can be assembled on the tips of the aligned nanowires in a few minutes (Figure 1). During the assembling process, more than one QD could be attracted to the tips of nanowire, which could result in larger and brighter QDs. In principle, these QDs could also form the pearl-chain structures on the tips of Au nanowires; however, it is difficult to directly confirm the pearl-chain formation via microscope

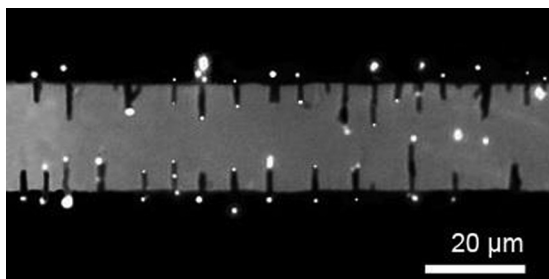


FIG. 1. Quantum dots can be precisely positioned on the tips of arrays of nanowires by the AC E -fields.

observation due to the ultrasmall diameters of QDs (<10 nm).

The assembling of QDs *cannot* be explained simply by the DEP effect. It is known that DEP force increases with the volume of objects.²⁷ By the DEP force alone, it is extremely inefficient to move QDs with a diameter less than 10 nm over a region of tens of micrometers, where estimation shows that the speed of QDs should be only a few nm/s.²⁰ Although the ultrafine tips of Au nanowires can enhance the E -field in their vicinities substantially, such an effect is highly localized and effective only in the vicinity of nanowires (supplementary materials S2).²⁰ A different electrokinetic mechanism other than the DEP force must be playing a role in circulating QDs around the edges of the microelectrodes, which brings QDs closer to the nanowires.

Among many electrokinetic phenomena, the alternating current electroosmosis (ACEO) effect drew our attention. ACEO results in electroosmotic flows circulating around microelectrodes due to the interactions of the E -field and the electrical double layers next to the electrodes. The fluid velocity in the horizontal direction is given by²⁸

$$v_{fluid} = \epsilon_m V_{rms}^2 / \left[\eta (1 + \delta) L \left(\frac{\omega}{\omega_c} + \frac{\omega_c}{\omega} \right)^2 \right], \quad (2)$$

where V_{rms} is the root mean square of applied voltage; ϵ_m and η are the permittivity and viscosity of the suspension medium; L is the electrode spacing; δ is the capacitance ratio of the diffusion and compact layers (assumed as constant for both); ω_c and ω are the peak and applied E -field frequency, respectively. The movement pattern of QDs exhibits a great similarity with that of nanoparticles under the influence of ACEO effect (Figure 2(a)).^{20,29-31}

To confirm that the circulating motion of QD is indeed due to the ACEO effect, we characterized the velocities of QDs as a function of the applied voltages from 5 to 20 V at

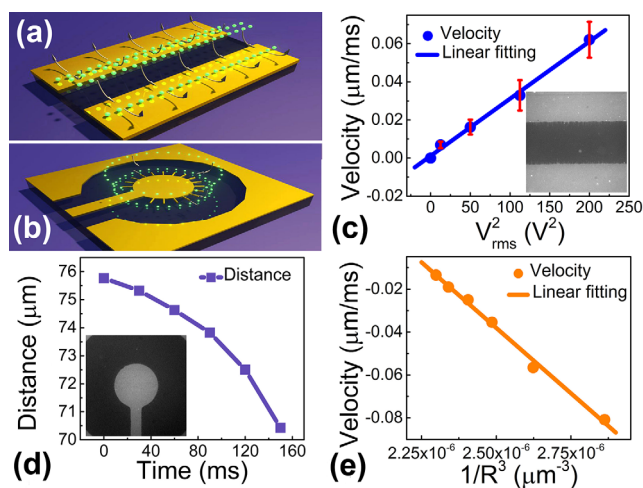


FIG. 2. (a) Schematic diagram of ACEO flows for QD manipulation. (b) Schematic diagram of manipulation QDs in the circular microelectrodes. (c) The velocities of QDs linearly increase with V_{rms}^2 , inset: snapshot of QD movement due to ACEO flows. (multimedia view). (d) Distance of a QD to the center of the inner electrode versus time. Inset: snapshot of the circular microelectrode. (e) Velocity of QD increases linearly with $1/R^3$. (Multimedia view) [URL: <http://dx.doi.org/10.1063/1.4893878.1>] [URL: <http://dx.doi.org/10.1063/1.4893878.2>]

50 kHz. The velocities were determined from QDs on the top of the parallel microelectrodes. The velocities linearly increase with V_{rms}^2 (Figure 2(c)), agreeing with the relation of $v \sim V_{rms}^2$ given in Eq. (2). However, it remains difficult to attribute the high precision assembling of QDs on the tips of nanowires (only 300 nm in diameter) to the ACEO effect.

It is noted that for nanowires attached on parallel microelectrodes in an external E -field, the E -field strength can be substantially enhanced in the vicinity of the tips of nanowires, which result in a high E -field gradient as shown in the simulation in supplementary materials S2.²⁰ The attraction of small objects to the highest E -field gradient is a hallmark of positive DEP forces.^{22,23} Our quantitative study of the transport of QDs to the tips of nanowires confirmed such an effect.

Since there is no analytical solution of the E -field distribution around a nanowire, we designed a pair of concentric microelectrodes with inner and outer radii of 65 μm and 200 μm , respectively (Figure 2(b)). In such a microelectrode, the DEP force (F_{DEP}) can be analytically obtained, which is proportional to $1/R^3$, given by $F_{DEP} \sim \nabla E^2 \sim 1/R^3$ according to Eq. (1), where R is the distance of the nanoobjects to the center of the inner electrode. After attaching the nanowires to the edge of the inner electrode at 70 kHz and 20 V, QDs can be readily assembled on the tips of the nanowires (90 kHz and 20 V) (Figure 2(d)).²⁰ To clearly determine the nature of the attraction force, we analyzed the motions of QDs when they were a few micrometers away from the tips of nanowires. We consistently found that the velocities of such QDs ($|v|$) linearly increase with $1/R^3$ (Figure 2(e)).²⁰ Given that the viscous drag force (F_{drag}) instantly balances the applied external forces, i.e., $F_{DEP} \approx F_{drag} \sim v$, for nanoparticles in the extremely low Reynolds number regime, the as-observed $v \sim 1/R^3$ accounts for the dependence of $F_{DEP} \sim 1/R^3$.²⁴ This analysis confirms that the attraction force received by the QD is the DEP force. As a result, the entire assembling process of QD-on-nanowires can be understood quantitatively, where the QDs in the suspension were coherently moved on top of the microelectrodes largely due to the ACEO influence, when they were brought close to the nanowires, the DEP force around the tips of nanowires dominated, attracting and positioning them precisely on the tips of nanowires. This result agrees with previous work on sole QD manipulation,²⁶ but was achieved in a nanowire-QD system and confirmed in a direct and quantitative manner. Also note that the assembling of QD-nanowire hybrid is highly facile and controllable, which took just seconds to minutes depending on the concentration of QDs.

The QD-nanowire assemblies were applied for position deterministic biochemical sensing, where the nanowires defined the positions of the QD biosensors. Note that in the aforesaid study, regardless of the applied AC frequencies, the nanowires attached on the edge of microelectrodes were *not* assembled in an order array (supplementary material S1).²⁰ We also notice that the fluorescent intensity of QDs and organic dyes can be quenched significantly if they directly contact metal surfaces.³² To resolve these two issues before demonstrating the QD-nanowire assemblies for sensing applications, the surfaces of microelectrodes and Au nanowires were modified with a thin layer of PMMA

(MicroChem 950 k C2, ~ 200 nm in thickness) and silica (40 nm), respectively.²⁰ The presence of the thin PMMA layer can maintain the mobility of Au nanowires attaching on the edges of the microelectrodes and result in an equally spaced nanowire array due to the electrostatic repulsion between neighboring nanowires in an AC E -field (Figure 3).³³ The separation between QDs and metal nanowires by the silica coating can precisely tune the fluorescent enhancement of QDs due to the plasmonic Au nanowires, which will be discussed elsewhere.³⁴ With the above consideration and modification, we obtained an array of evenly spaced QD-nanowire devices under E -field at 20 V, 700 kHz. The average distance between neighbored QD-nanowire assemblies was ~ 8.5 μm for a nanowire suspension of $2.2 \times 10^7/\text{ml}$ and QDs of 0.1 nM (Figures 3(a) and 3(b)).

The as-obtained QD-nanowire assemblies were demonstrated as nanosensors for detection of biomolecules. Biotin molecules, bonding strongly with streptavidin, are commonly used for device demonstrations.³⁵ In the experiments, after assembling QDs conjugated with streptavidin (0.1 nM, emission: 605 nm, Invitrogen Inc.) on the tips of nanowires in an AC E -field of 20 V and 700 kHz, Cy5-labeled biotin molecules (200 nM, 4 μl , Nanocs Inc.) were introduced in the same AC E -field. In a few minutes, the characteristic fluorescent signals of Cy5-biotin can be detected on the tips of nanowires, co-localized with that of QDs (Figures 3(a) and 3(b)). When the concentration of Cy5-biotin was reduced to only 20 nM, there were still 52.6% QD on the tips of nanowires showed the co-localized signals of Cy5-biotin. Note that the co-localization of QDs and biotin occurred in just a few minutes after the application of the E -field, which is much faster than those demonstrated previously, where a

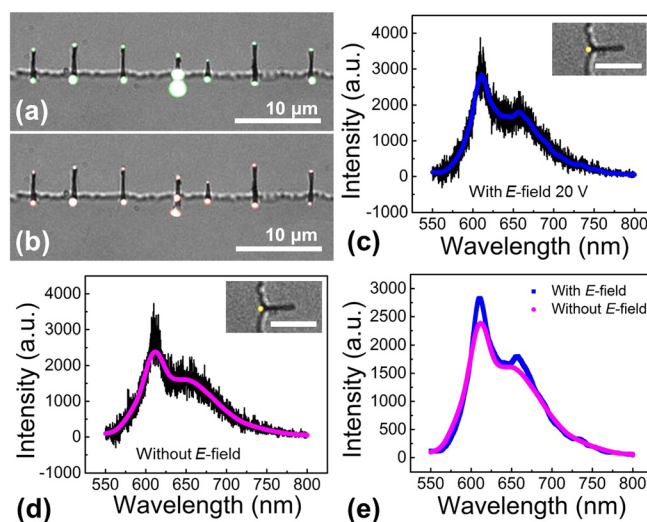


FIG. 3. Under an AC E -field (700 kHz, 20 V), Cy5-biotin molecules can be efficiently focused on the tips of nanowires in suspension, co-localized with QDs coated with streptavidin for enhanced biodetection. (a) Fluorescent images of QDs on an array of assembled Au nanowires taken through a band pass filter of 605 nm (585 nm to 625 nm). (b) Fluorescent images of Cy5-biotin molecules on the same arrays of Au nanowires taken through a 650 nm long pass filter. Fluorescent spectra taken on the nanowire tips when the AC E -field is (c) on and (d) off, demonstrating the effective E -field focusing and specific conjugation of QD and Cy5-biotin. The insets show the corresponding fluorescent images with pseudocolors. The scale bar is 5 μm . (e) The signals of QD and Cy-5 biotin with/without the E -field.

conjugation time of at least 30 min has to be taken before signals of both molecules can be successfully detected.^{36,37} This suggests that the DEP force not only assemble QDs on the tips of nanowires as aforesaid, but also could focus biomolecules, such as biotin, to the tips of nanowires to enhance the detection efficiency.

To confirm this understanding, we performed a series of control experiments. Cy5-labeled biotin of various concentrations from 200 pM to 20 pM was introduced to a simple array of assembled nanowires (without presence of QDs) at 700 kHz and 20 V. In a few minutes, biotin could be readily detected at the tips of nanowires from both the fluorescence imaging and spectroscopy of Cy5 (supplementary material S4). This experiment showed that indeed analyte molecules can be concentrated at the tips of nanowires due to the AC E -field.

It is critical to know if the molecules co-localized with QDs are the sought-after biotin molecules, which should specifically bond to the streptavidin-coated QDs. After incubation for 30 min, the E -field was carefully removed to release the non-specific molecules. Most QD-nanowire assemblies still remained (90%), which could be due to the non-specific bonding of functionalized QDs and nanowire tips. For a Cy5-biotin concentration of 20 nM and in 15 tested devices, after the E -field release, 55.6% QD-nanowires retained the original co-localized Cy5 signals with a slight decrease in the intensity of both QDs and Cy5-biotin (Figure 3(e)). In comparison, at the same condition, if by using bare QDs without streptavidin (QD 525), majority of Cy5 labeled biotin disappears from the QDs on the tips of nanowires after the E -field release (Figure 4). Only $\sim 14.3\%$ QDs retained the original signals of Cy5-biotin, which is substantially lower than that obtained from the streptavidin coated QDs (55.6%). This result demonstrates that the QD-nanowire system can detect desirable molecules due to the specific conjugation between QDs and the analyte molecules.

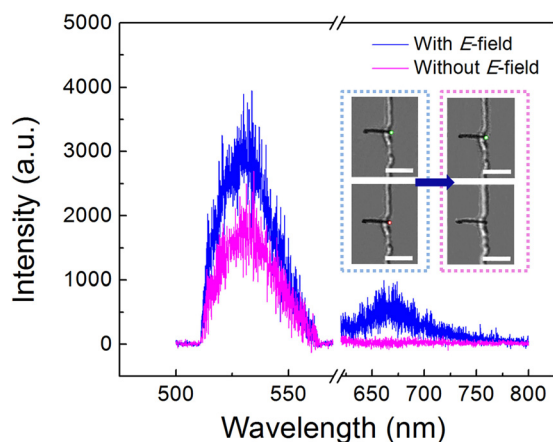


FIG. 4. Control experiments: under the AC E field (700 kHz, 20 V), fluorescent spectrum (in blue) shows both QDs (without streptavidin, emission: 525 nm, 535 nm band pass filter from 505 nm to 560 nm) and Cy5-biotin molecules (emission 670 nm, 532 nm long pass filter) at the tips of nanowires. After removal of the AC E -field, the signal of Cy5-biotin disappeared due to the detachment from the QDs (in magenta). Inset on the left: fluorescent images showing both QDs and Cy5-biotin under the AC E field. Inset on the right, fluorescent images after removal of the E field.

As a result, the QD-nanowire sensors operate uniquely by effectively focusing molecules to QDs before detection via specific conjugation. In comparison, if we directly incubate streptavidin conjugated QDs, spin coated on a glass substrate, with Cy5-biotin (20 nM) and detect the co-localized signals at the same conditions, only 17.2% signals showed the conjugation of QD and Cy5, which is much lower than that obtained from the QD-nanowire assemblies. The control experiments further confirm that our devices offer improved biodetection sensitivity (or efficiency) in addition to the merit of location-predictability. The improvement could be largely attributed to the concentration effect for both QDs and biotin due to the E -field. We also note that the plasmonic enhancement from the Au nanowires may improve the detection performance, which will be studied elsewhere.³⁴

The devices demonstrated here could inspire new strategies for resolving the intrinsic problem of low throughput of nanosensors.³⁸ With further investigation and optimization, i.e., application of the 3D electrodes instead of 2D planar electrodes,^{39,40} integration with a microfluidic device, automation of optical analysis, and use of multiple functionalized QDs, the QD-nanowire assemblies could detect various analyte molecules in a rational, sensitive, multiplex, and efficient manner. Among all the aforementioned improvements, it is especially interesting to assemble the nanowire-QD hybrid sensors into 3-D structures in the detection system. The 3-D assembling scheme can enhance the detection efficiency substantially owing to the more effective interaction and focus of analyte molecules to the sensing areas compared to that of the 2-D scheme. This could be achieved by generating E -fields from designed 3-D electrodes, i.e., those made of a stack of insulator-separated plenary metals. Also note that based on our understanding of the ACEO effect, pressure driven flows, which bring the QDs to the vicinity of the nanowires, could also be employed to assist the assembling of the QD nanosensors owing to the same mechanism as that of the ACEO flows. However, the rate of the pressure driven flows should be controlled so that the hydrodynamic force is lower than the DEP force. Finally, the electric-field assisted QD assembly has its own limitation compared to the previous work,³ where pattern microelectrodes are indispensable, which requires additional engineering and optimization when integrating with other systems, e.g., microfluidics.

In summary, QDs with a diameter of <10 nm were precisely manipulated and assembled on tips of Au nanowires. The manipulation mechanism was understood quantitatively and attributed to a synergetic ACEO and DEP effect. After modification of the surfaces of the microelectrodes and Au nanowires, the QD-nanowire assemblies can be arranged in an equally spaced array and demonstrated for biochemical detection. The device operated uniquely by focusing analytes to the QD nanosensors before detection via specific biochemical conjugation. Molecules, such as biotin, can be detected unambiguously in a location deterministic manner with much enhanced efficiency. With further investigation and optimization, such devices could potentially be integrated with microfluidics for position deterministic biochemical sensing. The outcome of this research may not only advance the QD-based sensing technology, but also inspire a

potentially scalable approach for fabricating various QD-based nanodevices.

We are grateful for the support from National Institutes of Health (9R42ES024023-02), Welch Foundation (Grant No. F-1734). The work was also supported by National Science Foundation CAREER Award (Grant No. CMMI 1150767) in part, and UT-Austin startup package from the Cockrell School of Engineering.

- ¹X. H. Gao, Y. Y. Cui, R. M. Levenson, L. W. K. Chung, and S. M. Nie, *Nat. Biotechnol.* **22**, 969 (2004).
- ²W. C. W. Chan and S. M. Nie, *Science* **281**, 2016 (1998).
- ³C. Y. Zhang, H. C. Yeh, M. T. Kuroki, and T. H. Wang, *Nature Mater.* **4**, 826 (2005).
- ⁴H. H. Chen, Y. P. Ho, X. Jiang, H. Q. Mao, T. H. Wang, and K. W. Leong, *Mol. Ther.* **16**, 324 (2008).
- ⁵C. L. Grigsby, Y. P. Ho, and K. W. Leong, *Nanomedicine-Uk* **7**, 565 (2012).
- ⁶X. Michalet, F. F. Pinaud, L. A. Bentolila, J. M. Tsay, S. Doose, J. J. Li, G. Sundaresan, A. M. Wu, S. S. Gambhir, and S. Weiss, *Science* **307**, 538 (2005).
- ⁷R. Wilson, A. R. Cossins, and D. G. Spiller, *Angew. Chem. Int. Ed.* **45**, 6104 (2006).
- ⁸J. M. Klostranec, Q. Xiang, G. A. Farcas, J. A. Lee, A. Rhee, E. I. Lafferty, S. D. Perrault, K. C. Kain, and W. C. W. Chan, *Nano Lett.* **7**, 2812 (2007).
- ⁹T. Pellegrino, W. J. Parak, R. Boudreau, M. A. Le Gros, D. Gerion, A. P. Alivisatos, and C. A. Larabell, *Differentiation* **71**, 542 (2003).
- ¹⁰W. B. Cai, A. R. Hsu, Z. B. Li, and X. Y. Chen, *Nanoscale Res. Lett.* **2**, 265 (2007).
- ¹¹I. L. Medintz, A. R. Clapp, F. M. Brunel, T. Tiefenbrunn, H. T. Uyeda, E. L. Chang, J. R. Deschamps, P. E. Dawson, and H. Mattoussi, *Nature Mater.* **5**, 581 (2006).
- ¹²W. R. Algar, M. G. Ancona, A. P. Malanoski, K. Susumu, and I. L. Medintz, *ACS Nano* **6**, 11044 (2012).
- ¹³V. Biju, D. Muraleedharan, K. Nakayama, Y. Shinohara, T. Itoh, Y. Baba, and M. Ishikawa, *Langmuir* **23**, 10254 (2007).
- ¹⁴M. Zhou, E. Nakatani, L. S. Gronenberg, T. Tokimoto, M. J. Wirth, V. J. Hruby, A. Roberts, R. M. Lynch, and I. Ghosh, *Bioconjugate Chem.* **18**, 323 (2007).
- ¹⁵Y. G. Kim, S. Moon, D. R. Kuritzkes, and U. Demirci, *Biosens. Bioelectron.* **25**, 253 (2009).
- ¹⁶Z. T. Deng, Y. Zhang, J. C. Yue, F. Q. Tang, and Q. Wei, *J. Phys. Chem. B* **111**, 12024 (2007).
- ¹⁷A. Karwa, E. Papazoglou, K. Pourrezaei, S. Tyagi, and S. Murthy, *Inflamm. Res.* **56**, 502 (2007).
- ¹⁸A. Zajac, D. S. Song, W. Qian, and T. Zhukov, *Colloid Surf. B* **58**, 309 (2007).
- ¹⁹I. L. Medintz, M. H. Stewart, S. A. Trammell, K. Susumu, J. B. Delehanty, B. C. Mei, J. S. Melinger, J. B. Blanco-Canosa, P. E. Dawson, and H. Mattoussi, *Nature Mater.* **9**, 676 (2010).
- ²⁰See supplementary material at <http://dx.doi.org/10.1063/1.4893878> for the details of sample preparations, experimental setup, estimation of QDs' velocity under the DEP effect, E-field distribution simulation, chaining effect of the nanowires, attraction of Cy5 molecules, and the movies for DEP effect and ACEO effect.
- ²¹D. L. Fan, F. Q. Zhu, R. C. Cammarata, and C. L. Chien, *Appl. Phys. Lett.* **89**, 223115 (2006).
- ²²H. A. Pohl, *Dielectrophoresis: The Behavior of Neutral Matter in Nonuniform Electric Fields* (Cambridge University Press, Cambridge, New York, 1978), pp. xii.
- ²³T. B. Jones, *Electromechanics of Particles* (Cambridge University Press, Cambridge, New York, 1995), pp. xxii.
- ²⁴D. L. Fan, F. Q. Zhu, R. C. Cammarata, and C. L. Chien, *Appl. Phys. Lett.* **85**, 4175 (2004).
- ²⁵K. Kim, F. Q. Zhu, and D. L. Fan, *ACS Nano* **7**, 3476 (2013).
- ²⁶M. L. Y. Sin, V. Gau, J. C. Liao, D. A. Haake, and P. K. Wong, *J. Phys. Chem. C* **113**, 6561 (2009).
- ²⁷A. Castellanos, A. Ramos, A. Gonzalez, N. G. Green, and H. Morgan, *J. Phys. D: Appl. Phys.* **36**, 2584 (2003).
- ²⁸D. Li, *Encyclopedia of Microfluidics and Nanofluidics* (Springer, New York, 2008).
- ²⁹C. C. Huang, M. Z. Bazant, and T. Thorsen, *Lab Chip* **10**, 80 (2010).
- ³⁰M. Z. Bazant and Y. X. Ben, *Lab Chip* **6**, 1455 (2006).
- ³¹S. Debesset, C. J. Hayden, C. Dalton, J. C. T. Eijkel, and A. Manz, *Lab Chip* **4**, 396 (2004).
- ³²E. Dulkeith, A. C. Morteaux, T. Niedereichholz, T. A. Klar, J. Feldmann, S. A. Levi, F. van Veggel, D. N. Reinhoudt, M. Moller, and D. I. Gittins, *Phys. Rev. Lett.* **89**, 203002 (2002).
- ³³M. W. Li, R. B. Bhiladvala, T. J. Morrow, J. A. Sioss, K. K. Lew, J. M. Redwing, C. D. Keating, and T. S. Mayer, *Nat. Nanotechnol.* **3**, 88 (2008).
- ³⁴C. Liu, P. F. Zhang, K. Kim, H. C. Yeh, J. H. Werner, and D. L. Fan, "Plasmonic enhancement of semiconductor nanoemitters on the tips of nanoantennas" (unpublished).
- ³⁵C. M. Niemeyer, *Bioconjugation Protocols: Strategies and Methods* (Springer, 2004).
- ³⁶D. S. Lidke, P. Nagy, R. Heintzmann, D. J. Arndt-Jovin, J. N. Post, H. E. Grecco, E. A. Jares-Erijman, and T. M. Jovin, *Nat. Biotechnol.* **22**, 198 (2004).
- ³⁷O. Lileg, M. Lopez-Garcia, C. Semmrich, J. Auernheimer, H. Kessler, and A. R. Bausch, *Small* **3**, 1560 (2007).
- ³⁸P. E. Sheehan and L. J. Whitman, *Nano Lett.* **5**, 803 (2005).
- ³⁹H. A. Rouabah, B. Y. Park, R. B. Zaouk, H. Morgan, M. J. Madou, and N. G. Green, *J. Micromech. Microeng.* **21**, 035018 (2011).
- ⁴⁰R. Martinez-Duarte, R. A. Gorkin III, K. Abi-Samra, and M. J. Madou, *Lab Chip* **10**, 1030 (2010).